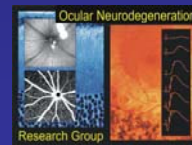# In *vivo*
assessment of ocular morphology
in animal models

Dr. Susanne C. Beck

Ocular Neurodegeneration Research Group

Institute for Ophthalmic Research

Schleichstr. 4/3, 72076 Tübingen

Universitäts-Augenklinik Tübingen

Ocular Neurodegeneration Research Group

Animal models in retinal degenerations

Retinal degenerations

→ A clinically and genetically heterogeneous group

→ so far untreatable degenerative diseases of the retina

→ includes stationary and progressive disorders of diffuse or localized nature

→ primarily retinal dystrophies

→ as well as secondary photoreceptor degenerations

→ due to defects of the pigment epithelium, the choroid, or systemic-metabolic diseases

Animal models

→ uncover the pathophysiology of ocular neurodegenerative processes

→ to develop and test therapeutic strategies and to understand and model normal retinal function

The basis is in-depth functional and morphological phenotyping of genetic models of blinding human neurodegenerative disorders with electroretinography (ERG), scanning-laser ophthalmoscopy (SLO), and optical coherence tomography (OCT) the same non-invasive techniques used in affected patients.

1

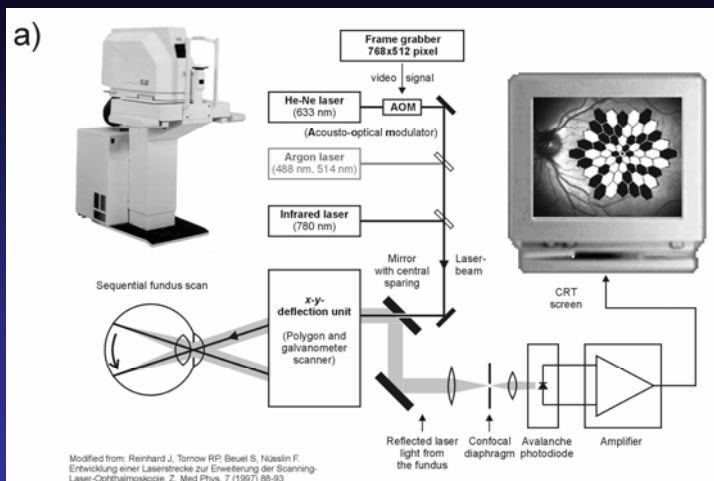# confocal Scanning Laser Ophthalmoscopy

---

Scanning laser ophthalmoscopy - principle

A laser beam is pre-shaped by a lens to be in focus at the retina.

The beam passes through a beam separator between the illuminating and reflected light.

The laser beam is then deflected horizontally as well as vertically to form a two-dimensional line scan raster.

The two-dimensional raster is focused to a single spot at the position of the eye´s lens and the optics of the eye then focuses this on to the retina.

Modified from: Reinhard J, Tornow RP, Beuel S, Nüsslin F. Entwicklung einer Laserstrecke zur Erweiterung der Scanning-Laser-Ophthalmoskopie. Z. Med Phys. 7 (1997) 88-93

The light reflected from the retina travels back along the same path as the illumination beam and is then descanned and collected by the beam separator and focused by a lens onto a photodetector, and can then either be recorded on video-tape or fed to a frame-grabber interfaced to a computer.

Scanning laser ophthalmoscopy – recording setup
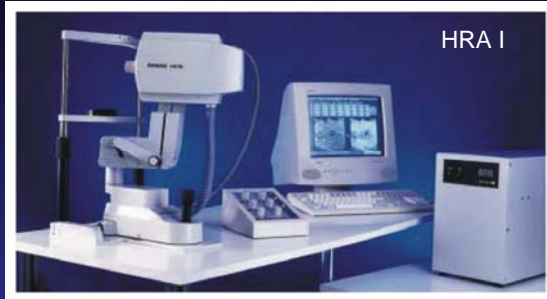

HRA I

Schematic drawing of an animal remarking the recording position on the XYZ table. The eye is directly facing the SLO recording unit.

The HRA1 is originally designed for diagnostic purposes in human. To use it for laboratory animals particularly mice we modified it for use with smaller eyes than humans.

The HRA1 is equipped with an argon laser in the short wavelength range and two diode infrared lasers in the long wavelength range.
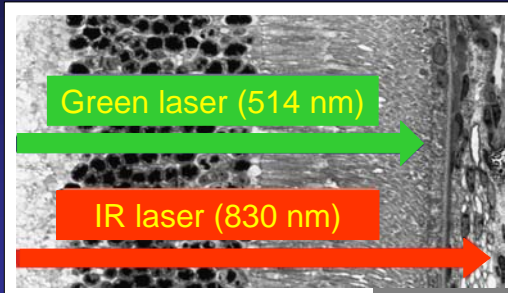
Scanning laser ophthalmoscopy of the eye
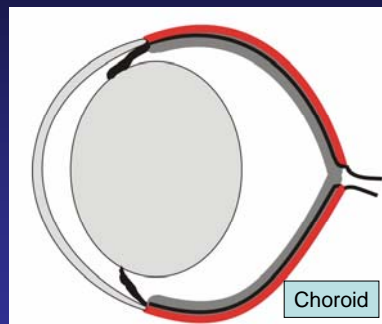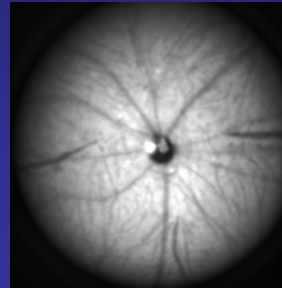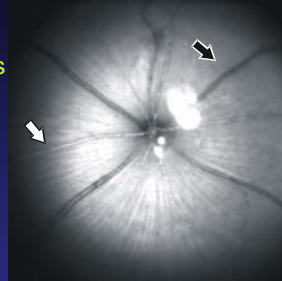

Choroid

Scanning laser ophthalmoscopy – native imaging

Argon laser:
- short wavelength: 514 nm
- more absorbed by melanin
- cannot penetrate RPE/choroid in pigmented animals
- high contrast images of retinal structures

Green laser (514 nm)
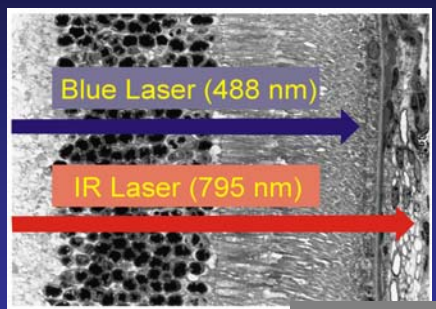
IR laser (830 nm)

RPE/Choroid

Infrared laser:
- long wavelength: 830 nm
- pass through pigmented layers
- less retinal details
- additional information about choroidal vasculature
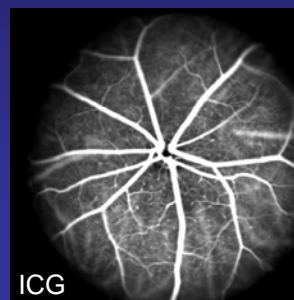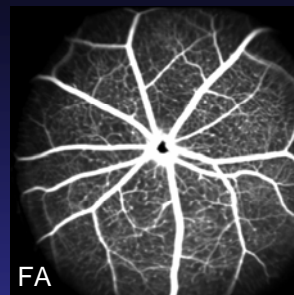
Scanning laser ophthalmoscopy – angiography

Argon laser:
- short wavelength: 488 nm, fluorescein
- cannot penetrate RPE/choroid in pigmented animals
- large retinal vessels
- best images of retinal capillaries

Blue Laser (488 nm)

IR Laser (795 nm)

RPE/Choroid

FA

ICG

Infrared laser:
- long wavelength: 795 nm, indocyanine green
- pass through pigmented layers
- less retinal details
- additional information about choroidal vasculature

Scanning laser ophthalmoscopy – „black versus white"

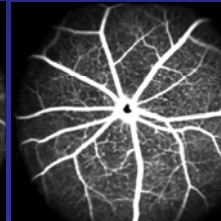**Visibility of deeper retinal structures depends directly on the amount of melanin in pigmented structures**

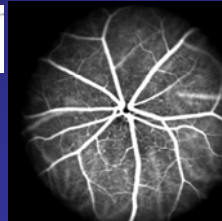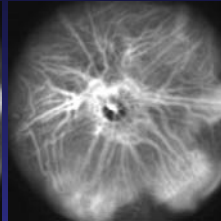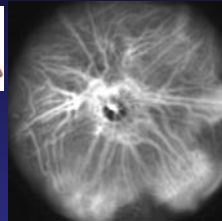ICG angiography   FA angiography

Degree of choroidal visibility:

- in a non-pigmented background best

- decreases with the amount of melanin

- lower in a strongly pigmented background like C57BL/6

BUT pigmented backgrounds have the advantage to allow a separation of retinal and choroidal systems by comparison of fluorescein and ICG angiography

---

Scanning laser ophthalmoscopy – anterior part of the eye

	Infrared laser		Green laser
		Angiography	
Cornea: - opaqueness - neovascularization	Native imaging 830 nm	Indocyanine green 795 nm	Fluorescein 488 nm
Iris: - pupillary reflex - iris vessels - fetal vasculature			
Lens - inclusions - opaqueness - cataract - fetal vasculature			
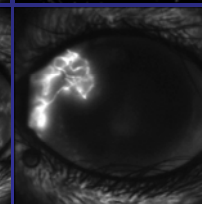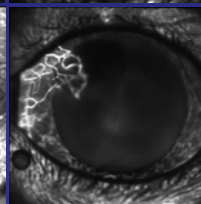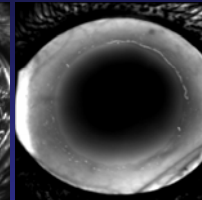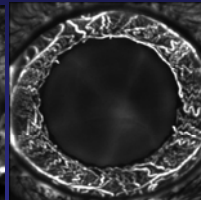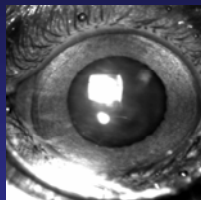
Cornea micropocket assay - a model for neovascularization

A micropocket is created in the cornea. A pellet is placed on the cornea and slid into the micropocket

Growth factor release from the pellet induces vessel growth from the limbus
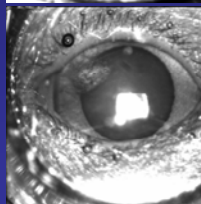

Cornea micropocket assay in cSLO imaging

cSLO assessment of vascular abnormalities in the anterior part of the eye

Cornea

Lens

Vitreous
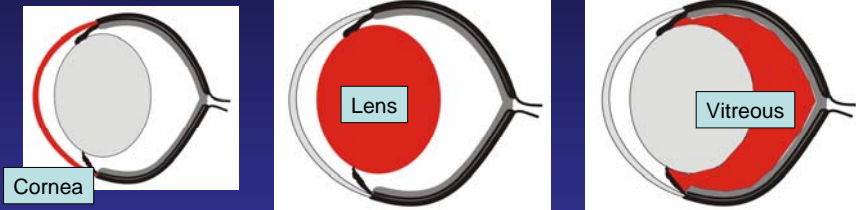
Vascular development in the eye

In mammalian eye development an intraocular vascular system nourish the developing eye when the retina is not yet vascularized

As the retinal vasculature develops the intraocular vessels regress

In humans, these vessel systems normally regress before birth,

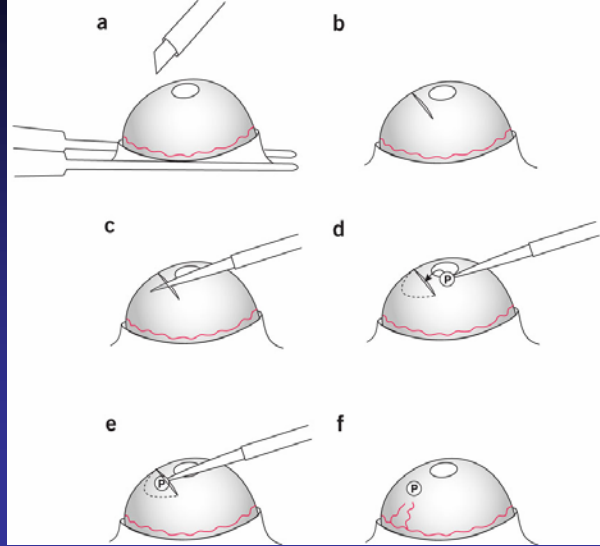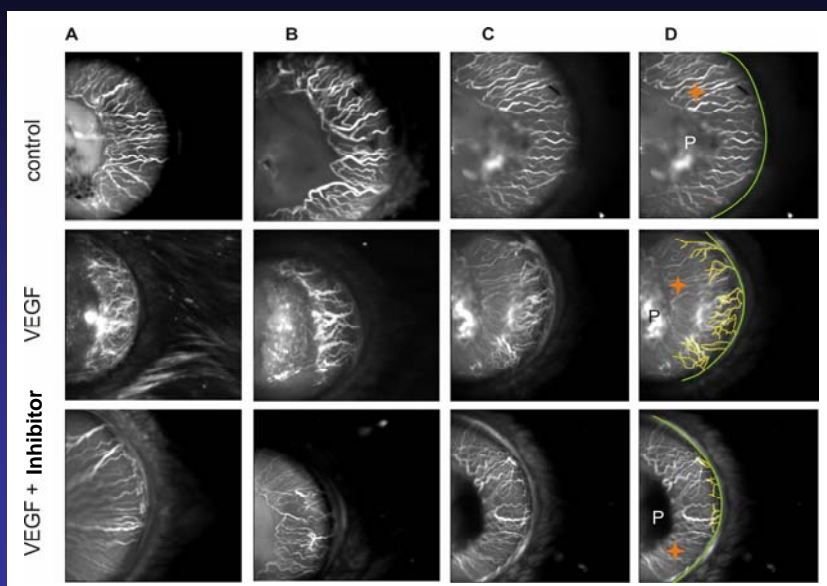**in mice and rats between 2 and 3 weeks after birth**

Iris

Pupillary membrane (PM)

Tunica vasculosa lentis (TVL)

Vasa hyaloidea propria (VHP)

Hyaloid artery (HA)

Retina

Optic nerve
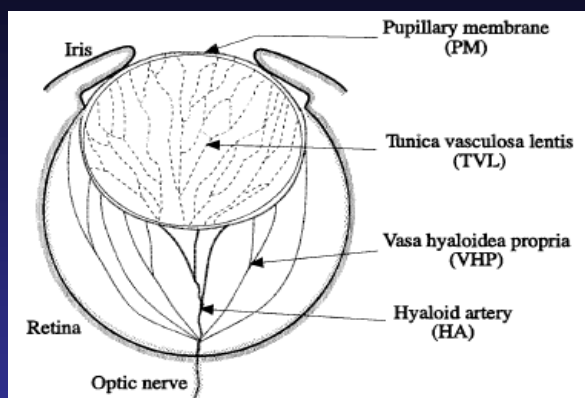
Fig. 1 Schematic diagram of the intraocular vessels in the mouse. Intraocular blood vessels consist of the pupillary membrane (*PM*), hyaloid arteries (*HA*), tunica vasculosa lentis (*TVL*), and vasa hyaloidea propria (*VHP*). In humans, these vessels disappear before birth

Ito, M. Anat Embryol (1999) 200:403–411

The anterior part of the eye is avascular

Retinal vascular development

Dorrell et al, Invest Ophthalmol Vis Sci 2002

Campochiaro & Hackett, Oncogene 2003

At birth retinal vasculature absent.
During the first three postnatal weeks, an adult vascular pattern is formed as endothelial cells migrate and proliferate from the central retinal artery toward the retinal periphery

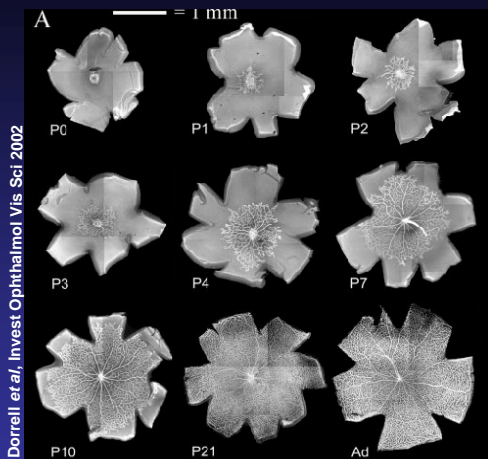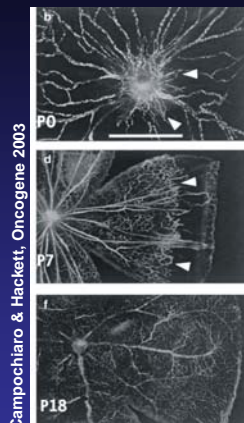**Fetal vascular system present during eye development.**
Concurrent with the growing vascular system the fetal vessels regress which supply the avascular periphery during development

Retinopathy of Prematurity - ROP
- a major cause of blindness in children

Immature lungs in preterm infants create a precarious respiratory status with risk of hypoxic injury to immature cells

Low oxygen

This is countered by administration of supplemental oxygen, both high and low oxygen levels are known to injure the immature photoreceptors

O$_2$

High oxygen

Incompletely vascularized retina

Premature infants have incompletely vascularized retinas, with a peripheral avascular zone The normal retinal vascular growth, which would occur in utero ceases, and there is loss of some of the developed vessels

Peripheral avascular zone of the retina

With maturation of the infant
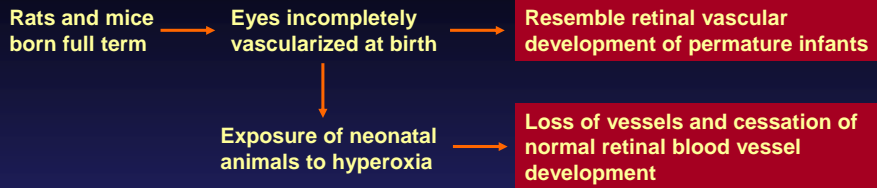
the retina becomes increasingly metabolically active

Hypoxic

Induction of formation of surplus abnormal vessels

Risk of retinal detachment and blindness

Induction of ROP in rats

Rats and mice born full term → Eyes incompletely vascularized at birth → **Resemble retinal vascular development of permature infants**

Eyes incompletely vascularized at birth → Exposure of neonatal animals to hyperoxia → **Loss of vessels and cessation of normal retinal blood vessel development**

mimics ROP

➡ **Different treatment schemes allow to generate a wide range of effects on the neural retina and the retinal vasculature that model the retinopathy, mild to severe, observed in human ROP**

50/10 model
- P0 to P14
- Alternating 24 hour periods of 50% and 10% oxygen
  - P14: returned to room air
- High oxygen at P0
- Rat retina is immature
- Blood oxgen levels mimic those experienced by preterm infants

75 model
- P7 to P14
- 75% oxygen
- High oxygen at P7
- Rat retina more mature
- Photoreceptors are differentiated as in the preterm infant

Induction of Retinopathy of Prematurity in Rats
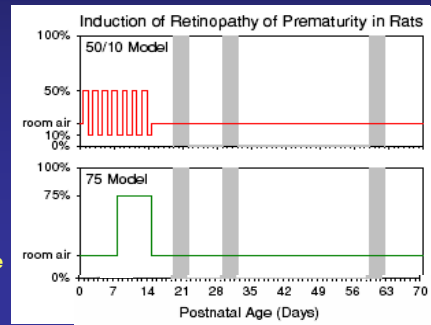
Fulton et al., Doc. Ophthal. 08

---

cSLO imaging of a rat model for human ROP

Time course analysis of the anterior eye segment in ROP rats

Control		ROP	
3 weeks	4 weeks	3 weeks	4 weeks
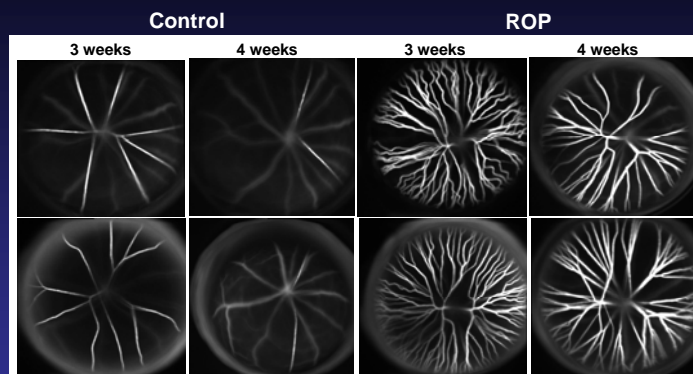
Blue laser stimulation using 488 nm wavelength after injection of fluorescein

To monitor the changes over a longer period of time, the same animal has been repeatedly analysed

Also in this pathologic conditions the vessels regress to a certain extent

cSLO imaging of the Norrie mouse

Norrie disease is a x-linked retinal dysplaisa that presents with congenital blindness, sensorineural deafness and mental retardation.
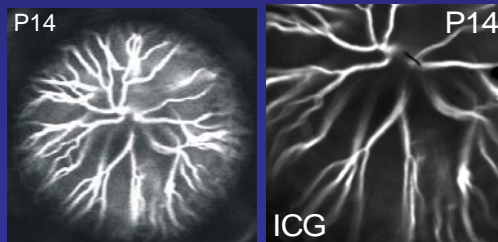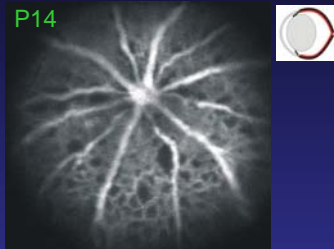
- Norrie KO mice show a distinct failure in retinal angiogenesis

- resulting in completely lack of the deep capillary layers of the retina

- only surface vessels can be formed, hypoxia of the inner retina results

- persistence of a large number of vitreal vessels

P14

P14

P14

ICG

---

cSLO imaging - detection of hyaloid vessels in mice
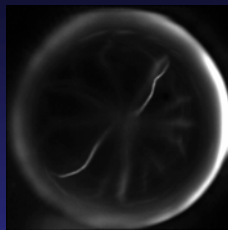
Hyaloid vessels in the mouse at 3 weeks of age

Regression of the fetal vasculature requires coordinated apoptosis and cell migration

Knock out of an extracellular matrix protein which is involved in cell migration results in persistent hyaloid vessels at 3 weeks of age

cSLO assessment of
retinal and choroidal vascular abnormalities

Cornea · Iris · Lens · Vitreous · Retina · Choroid

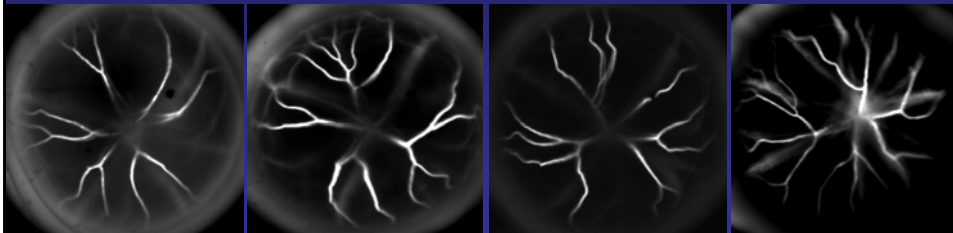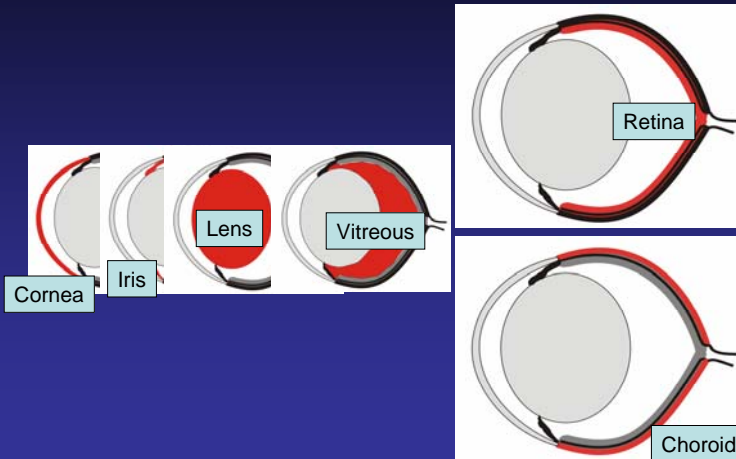## cSLO detection of retinal neovascularization

Retinal neovascularization processes are a major cause of vision loss in several retinal degenerative diseases, particularly wet **age-related macular degeneration** and **diabetic retinopathy**

Fenestrated vessels at sites of neovascularization can easily be **detected** using two different dyes and the appropriate laser wavelengths in **cSLO imaging**

Indocyanine green (ICG): long wavelength: 795 nm
Fluorescein (FLA): short wavelength: 488 nm

Blue Laser (488 nm)
IR Laser (795 nm)
RPE/Choroid
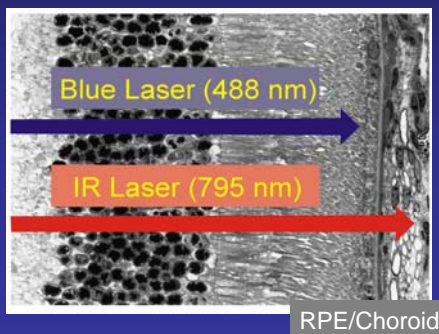
- Important difference: affinity to (large) plasma proteins

- ICG is bound to such proteins more than 98%

- FLA is only bound to about 60–80%

- ICG diffuses very slowly out of the vascular lumen even if vessels are fenestrated

- Fluorescein tends to leak rapidly

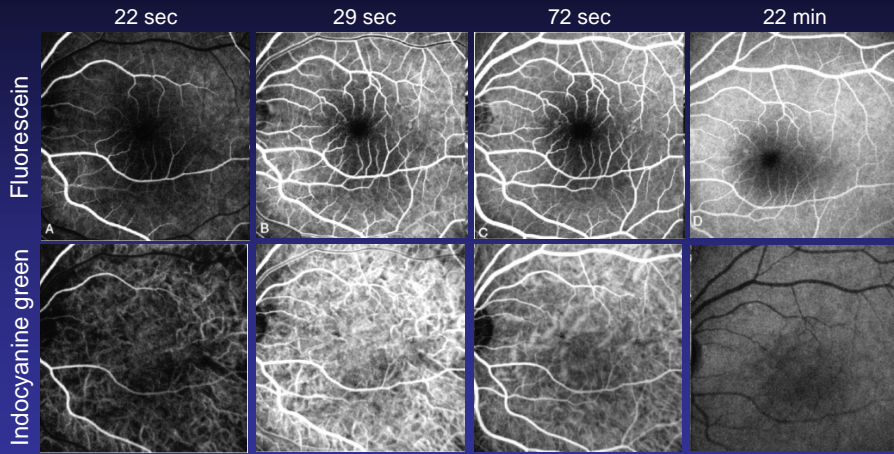# Angiography in human diagnostic

Fluorescein and ICG time course angiogram in a normal eye

Jorzik J.J., et al. Retina 25, 2005

Angiography in human diagnostic

Fluorescein and ICG angiography in age-related macular degeneration (AMD) with choroidal neovascularization
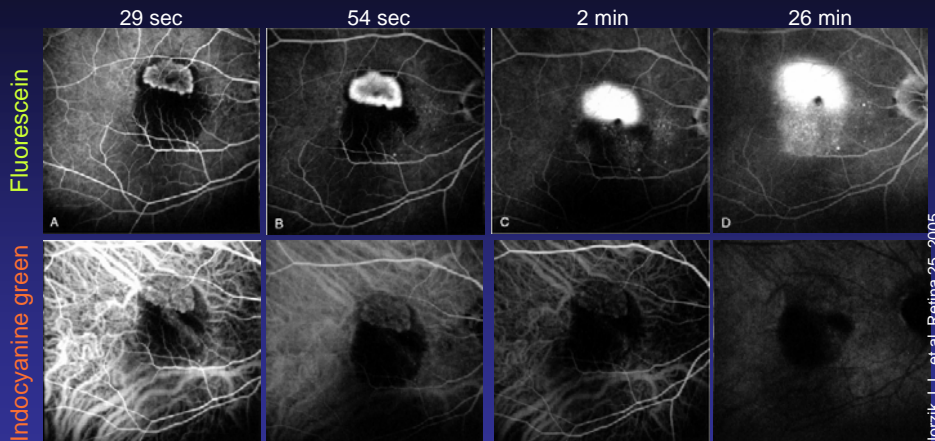
-FA angiography demonstrates the higher permeability of these choroidal vessels at the site of neovascularization
- FA leaks from rapidly from defective vessels which lead to a quick loss of image contrast, and the site of leakage turnes diffusely white
- ICG diffuses only very slowly out of the vascular lumen therefore gives still high-contrast images from the site of leakage

Jorzik J.J., et al. Retina 25, 2005

cSLO analysis of a mouse model for human exudative ARMD

Fluorescein: leakage in retinal neovascularisation
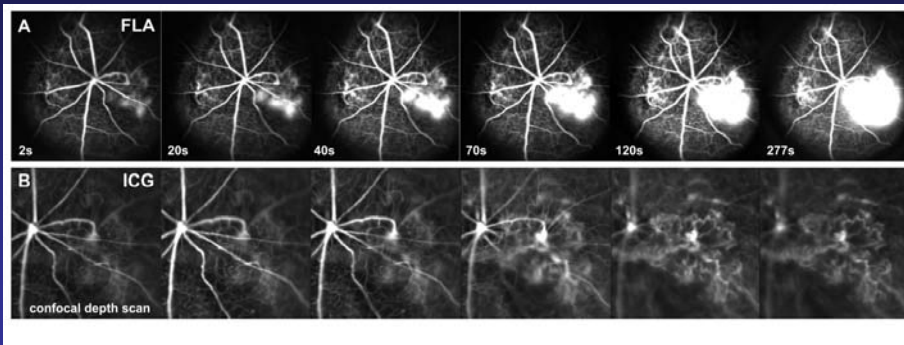
ICG imaging of subretinal membranes

---

cSLO fundus autofluorescence analysis

Short wavelength

514 nm   488 nm
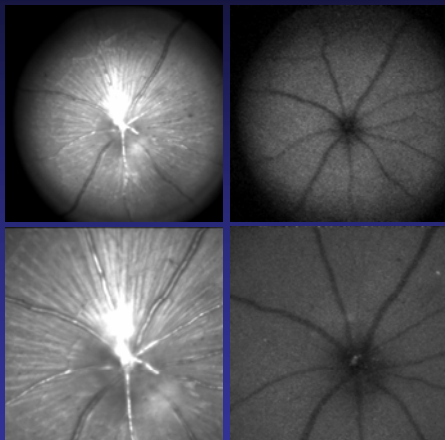
- **Fundus autofluorescence (FAF) is a relatively new technique for the detection of fluorophores like lipofuscin in retinal and RPE cells.**

- The normal fundus in FAF features a diffuse ''glow'' of lipids in retina and mainly RPE, which is blocked by the overlying vessels

- Enhanced autofluorescence indicates a pathological accumulation of lipids

- 488 nm detects also the jellyfish green fluorescent protein (GFP)

- **In mice, one can utilize the availability of transgenic models overexpressing (GFP) in different tissues**

13

cSLO FAF analysis in RPE65 knock out mice

FAF analysis 488 nm

RPE65 is an important protein of the visual cycle for the re-generation of rhodopsin

Deficiency in the gene for RPE65, leads to a metabolic block of this cycle in RPE cells

As a consequence, retinyl esters accumulate in the cells and form large lipid droplets

These droplets can easily be visualized in FAF imaging with 488 nm
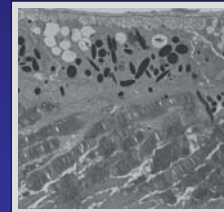
Control   RPE65-/-

In humans, mutations in the gene encoding RPE65 causes LCA2, a major form of Leber's congenital amaurosis, which lead to severe vision loss or blindness. First clinical trials for gene therapy are currently ongoing.
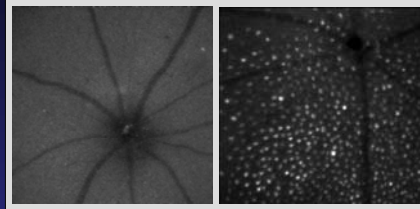
EM analysis

In vivo detection of GFP expression

The RG-GFP mouse

Histological sections

GFP expressed under control of a RG (cone) opsin promotor allows specific labelling of cone cells

In sections of 8 week old mice strong GFP expression can be selectively detected in cone photoreceptor cells

Single cone cells can be visualized in vivo using the autofluorescence mode with the 488 nm laser stimulus

Here In the highest magnification, single GFP-expressing cones are visible similar to a whole-mount preparation with transducin cone-specific staining

FAF 488 nm

wt

Gnat2
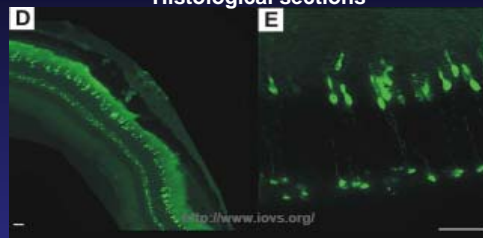
Beck et al., IOVS, 2010, Vol. 51, No. 1, 493.

In vivo detection of GFP expression

Repetitive examination of the same individual RG-GFP mice allows generation of a time course of GFP expression

3 weeks **4 weeks** **6 weeks** **8 weeks**

GFP expression reflects MWS opsin expression gradient

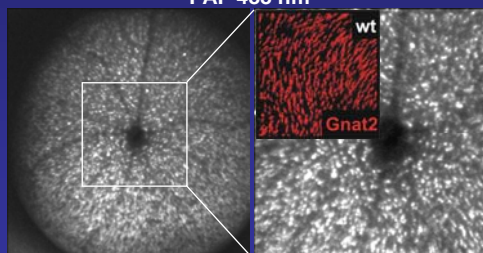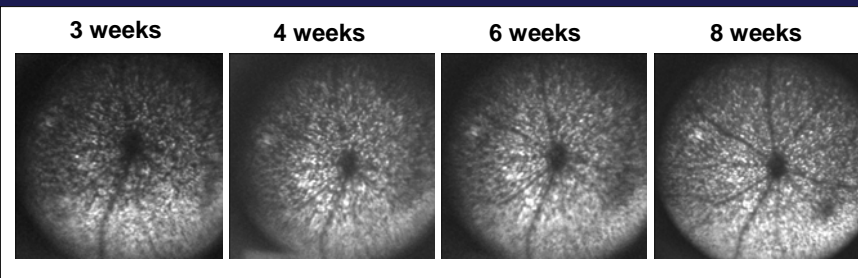In the RG-GFP animals GFP expression remains constant between 3 to 8 weeks of age

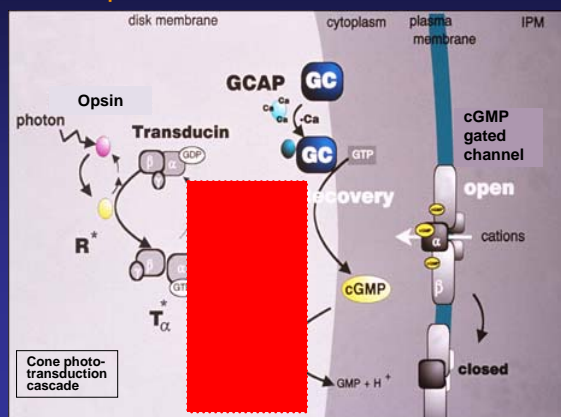Analysis of cone survival in animal models for retinal degeneration

MWS

An animal model for human achromatopsia: the cpfl1 mutant mouse

Cone dystrophies or also termed achromatopsia are a very important group of inherited retinal degenerations, different genes have been linked to achromatopsia and very recently the PDE6C gene

The cpfl1 mouse mutant which has a natural mutation in the PDE6C gene can be used for analysis of neurodegenerative processes in achromatopsia

116 bp insertion in the cGMP-phosphodiesterase a- subunit (PDE6C) gene of the cone photoreceptor causes failure of the phototransduction cascade

The mutated phospho-diesterase cannot hydro-lyse cGMP and thus the cGMP gated channel cannot be closed causing inhibition of the signalling of the light stimulus to adjacent neurons

disk membrane   cytoplasm   plasma membrane   IPM

GCAP   GC

Opsin

photon

Transducin

GC   GTP

cGMP gated channel

open

R*

cations

cGMP

T*

Cone photo-transduction cascade

GMP + H⁺   closed

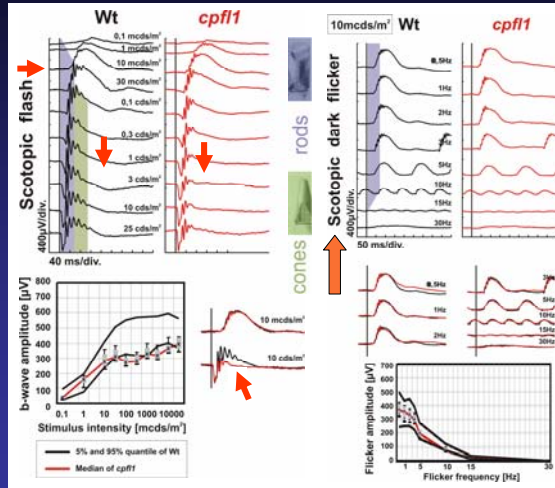**cone photoreceptor function loss (cpfl)**

The cpfl1 mutant mouse: in vivo functional analysis using ERG recordings

In scotopic flash ERG with increasing light intensities no differences are detectable up to 10 millicandelar, between Wt and CPFL1 mice

With higher intensities the cone contribution to the responses increases

About 10 candelar and more the response is strongly reduced in the CPFL1 mice (overlay)

Scotopic flicker ERG with 10 mcd intensity revealed that the rod system in the cpfl1 mouse is not affected. The responses from the rod system showed no alterations compared to WT mice

---

The cpfl1 mutant mouse: in vivo functional analysis using ERG recordings

In scotopic standard flicker ERG the responses decrease dramatically with increasing contributions of the cone system in cpfl1 mice

In the photopic flash ERG where mainly cones are responding almost no signal can be recorded
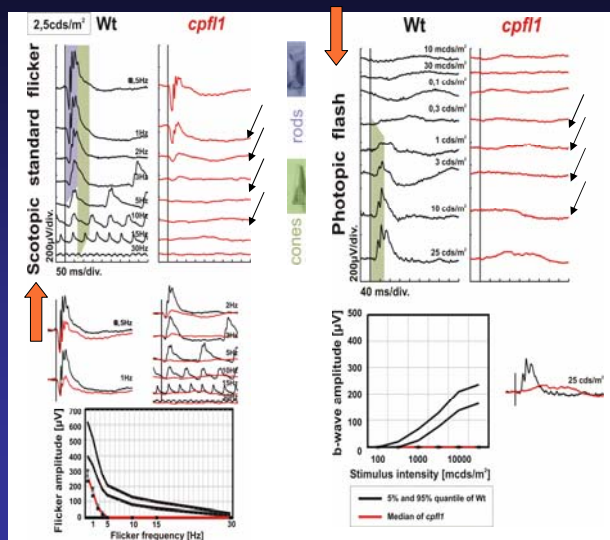
SLO analysis of *cpfl1* mice – native imaging and angiography

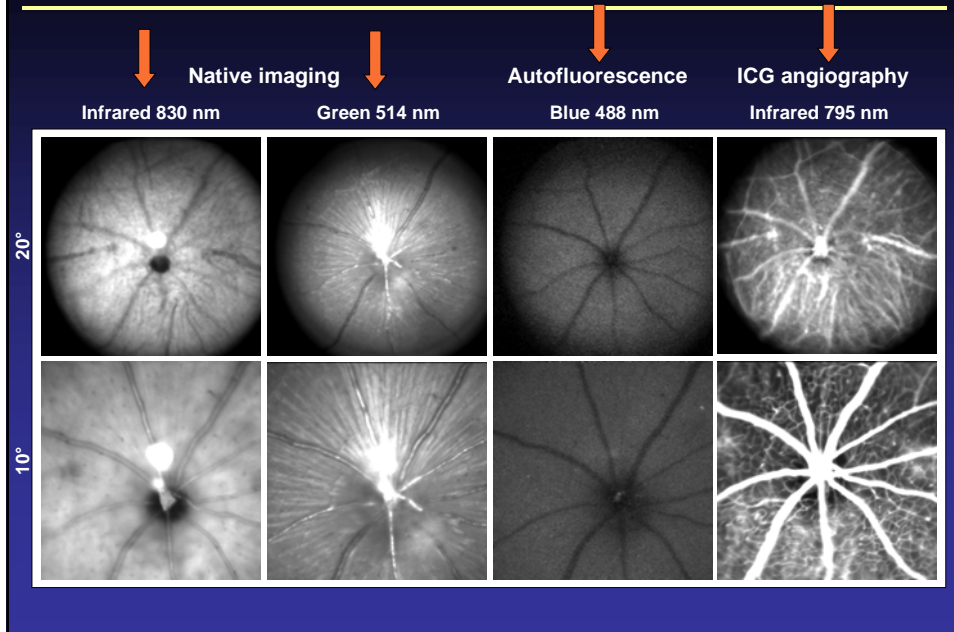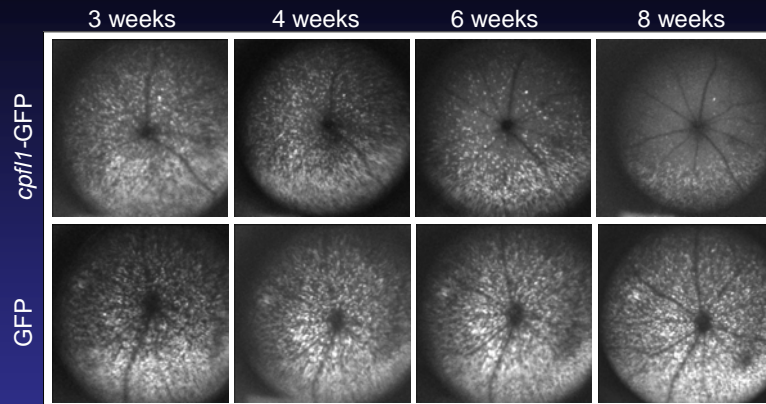|	Native imaging		Autofluorescence	ICG angiography
	Infrared 830 nm	Green 514 nm	Blue 488 nm	Infrared 795 nm

20°

10°

Analysis of cone survival in cpfl1 mice

RG-GFP mouse expressing GFP in cone cells
were crossbred with cpfl1 mice to generate cpfl1-RG-GFP transgenes

cpfl1

RG-GFP

cpfl1-RG-GFP

Time course of GFP expression

| | 3 weeks | 4 weeks | 6 weeks | 8 weeks |

cpfl1-GFP

GFP

GFP expression reflects MWS opsin expression gradient

MWS
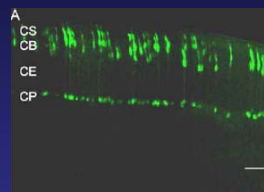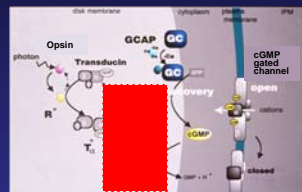
In cpfl1-GFP mice the GFP expression decreases considerably over time

Initially the doubly mutant displayed the same amount of GFP expression as their single RG-GFP counterparts but already at 4 weeks of age a reduction of GFP expression could be observed

After 8 weeks there was almost a complete loss of GFP expressing cells

The RG promoter limits the production of GFP protein to cones that also produce green (MWS) opsin, therefore in both mouse lines GFP is expressed with a dorsal-ventral gradient
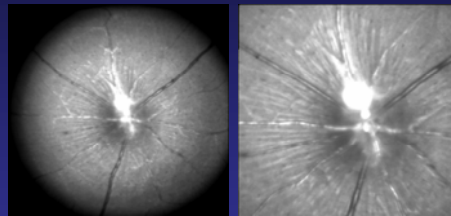
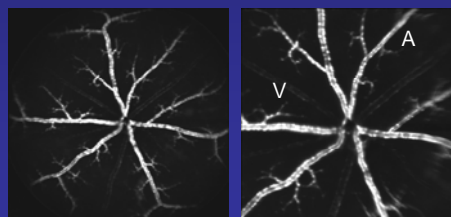Functional loss observed in ERG recordings is due to degeneration of cone photoreceptor cells

GFP expression in vascular endothelium: the SMA-GFP mouse

- GFP expression under the smooth muscle α-actin promotor
- specific for smooth muscle cells and contractile pericytes in blood vessels
- specific GFP labeling of the vessel wall

En-face imaging of retinal vessels using cSLO showed no apparent difference in the native red free mode (RF, 514 nm) between wild type and α SMA-GFP mice

In retinal whole mount preparation overlay of GFP expression and LectinTRITC labeling verify distribution of GFP expression in retinal arterioles and in the first and second order branches of the retinal arterioles.

Only few GFP positive cells are located at venules

FAF mode displays a strong GFP signal outlining retinal vessels in α SMA-GFP mice, in WT mice there is only the physiological background signal

Lectin
GFP

A

V
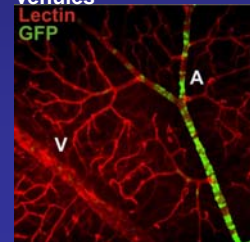
GFP detection in SMAA-GFP mice

C-SLO imaging of the ear

IR 830 nm   AF 488 nm

GFP detection in SMAA-GFP mice

C-SLO imaging of the hind leg

IR 830 nm   AF 488 nm toes   AF 488 nm sole of foot
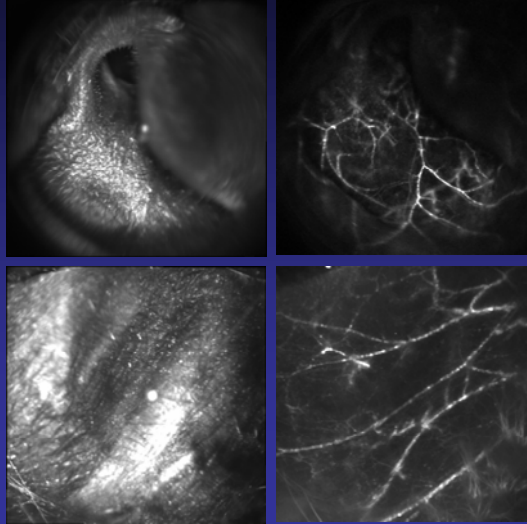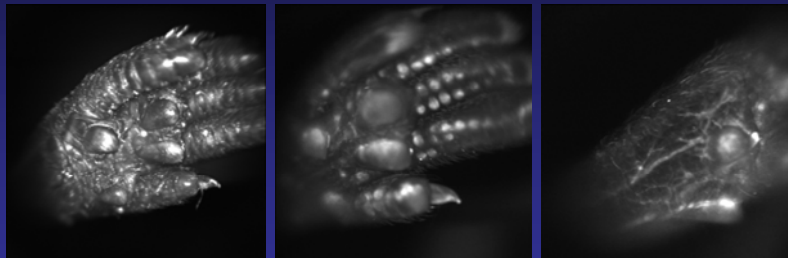
Detection of transplanted bone marrow-derived cells by GFP expression

irradiated

irradiated
head shielded

non irradiated

non irradiated

Cataract

irradiated

transplant

extract bone marrow cells
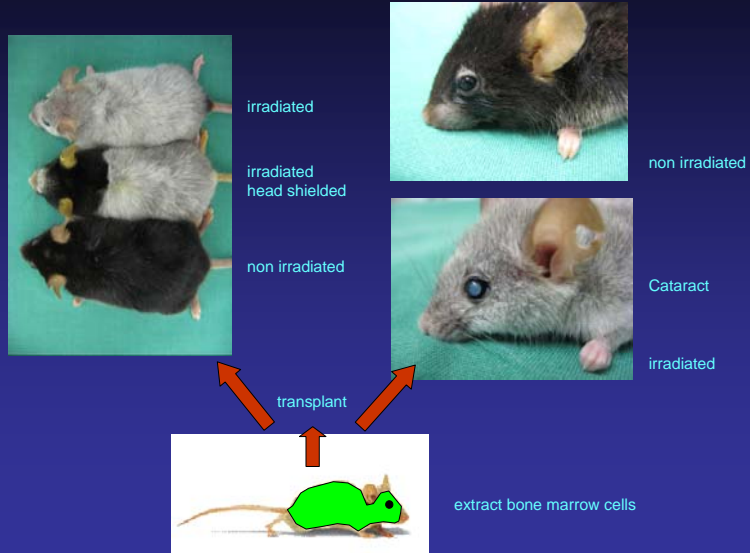
Detection of transplanted bone marrow-derived cells by GFP expression

Microglia shaped GFP cells in the retina are recgonized by CD11b suggesting that these cells are BM derived microglia, red are the endogenous microglia the green ones are the grafted from green bone marrow

CD11b

GFP

merge

allows detection of bone marrow-derived stem cells in vivo
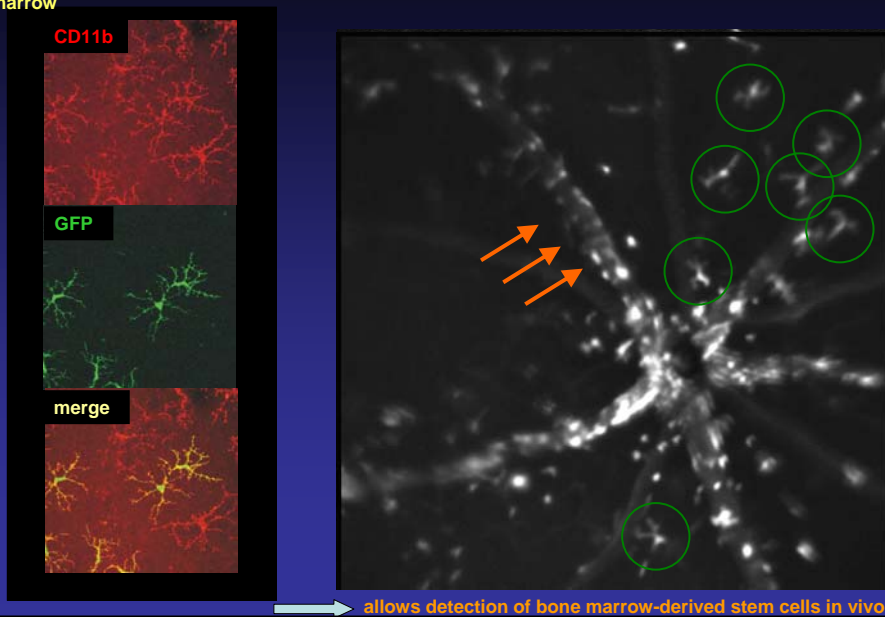
Spectral Domain
Optical Coherence Tomography

Optical coherence tomography

Conventional
Imaging

cSLO provides surface images

OCT

non-invasive testing of retinal morphology

provides high reso-lution depth profile based on reflectivity that correlates well with histomorphological sections
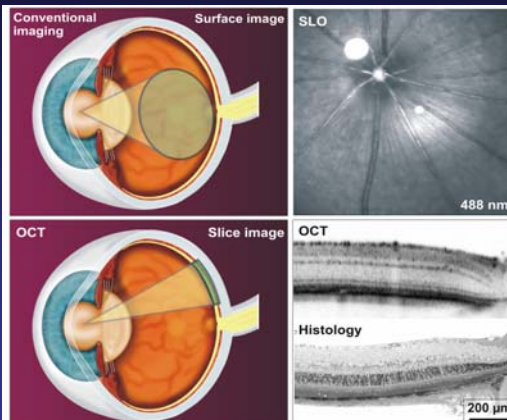
SD-OCT - principle

HE Spectralis HRA/OCT

40.000 A-scans/sec

Eye tracking

Noise Reduction
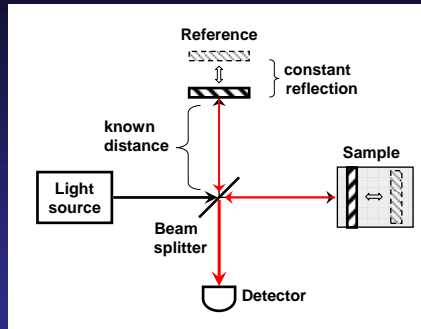
- Light split into sample & reference arm
- Sample and reference reflection create interference pattern
- Detector records interference pattern
- Variation of reference length yields different sample depths

---

Technical aspects

OCT (HRA Spectralis)

human
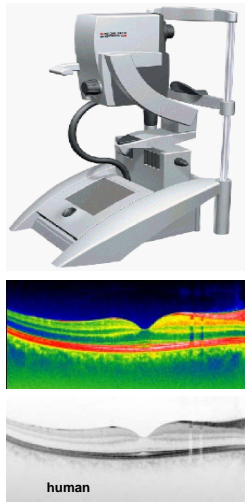
OCT recording setup for rodents

Schematic drawing of an animal remarking the recording position on the XYZ table. The eye is directly facing the OCT recording unit.

Correlation of reflexion sites and retinal layers

OCT images correlate well with histomorphological sections

Difference :
Histology is based on absorption (light shade - little absorption, dark shade - strong absorption)
OCT is based on reflectivity (light shade - weak reflectivity, dark shade - strong reflectivity)

Membranous surfaces are extremely well detected in OCT regardless of their physical extension

Membrane-rich but less optically dense layers like plexiform and nerve-fiber layers are represented in a darker shade of gray than optically more dense layers with less membrane content like the outer nuclear layer
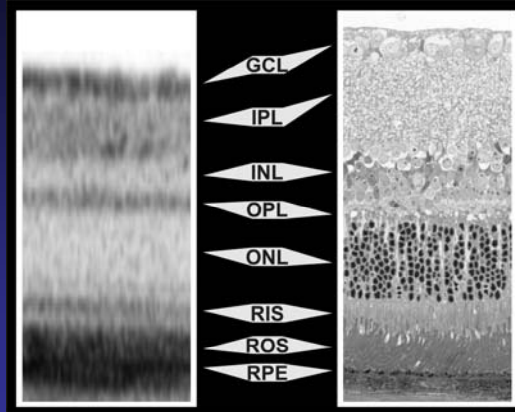
OCT provides not only refined depth resolution but also entirely new information about the sample structure

---

Retinal imaging in a normal BL6 mouse

Clear correlation between OCT and histology

Consecutive sections allow tracking of specific retinal structures

Relationship of OCT and histological morphometry in C57/Bl6

A

Comparison of retinal thickness in OCT and histology

High correlation of histological and OCT data demonstrated by:

Student's t-test: significance level p 0.05
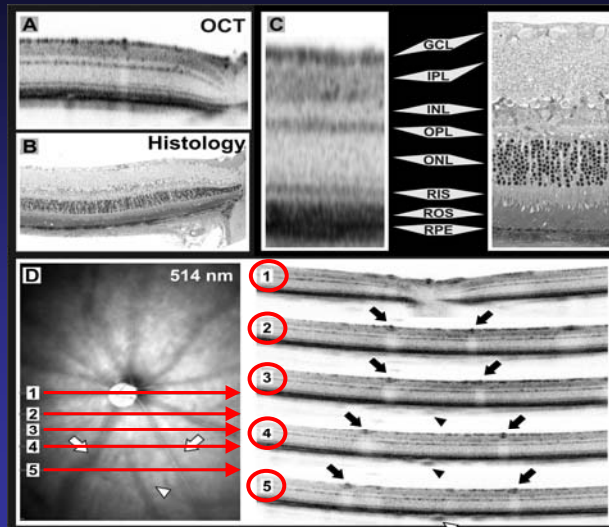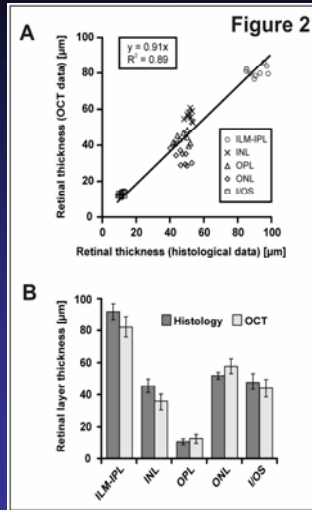
Best linear fit of the data yield a correlation coefficient R2 of 0.89

B

Comparison of retinal layer thickness between histological data and OCT

Average dimensions of the individual layers further confirm the close agreement between histology and OCT

No statistically significant difference between histological analysis and OCT-based quantification in any retinal layer

---

In vivo monitoring of progressive retinal degeneration

The RD1 mouse – an animal model for retinitis pigmentosa, autosomal recessive retinal degeneration, caused by loss-of-function mutation in the gene encoding the subunit of rod cGMP phosphodiesterase 6 (PDE6ß)

p10: TUNEL positive

p21: most rod photo-receptor nuclei have disappeared

p28: significant retinal degeneration
OCT showed an intact inner retina, whereas the inner nuclear layer (INL) seemed to border the RPE almost directly with the OPL/ONL, photo-receptor segments not detectable

En-face SLO imaging

p21   p35

SD-OCT cross-sectional imaging
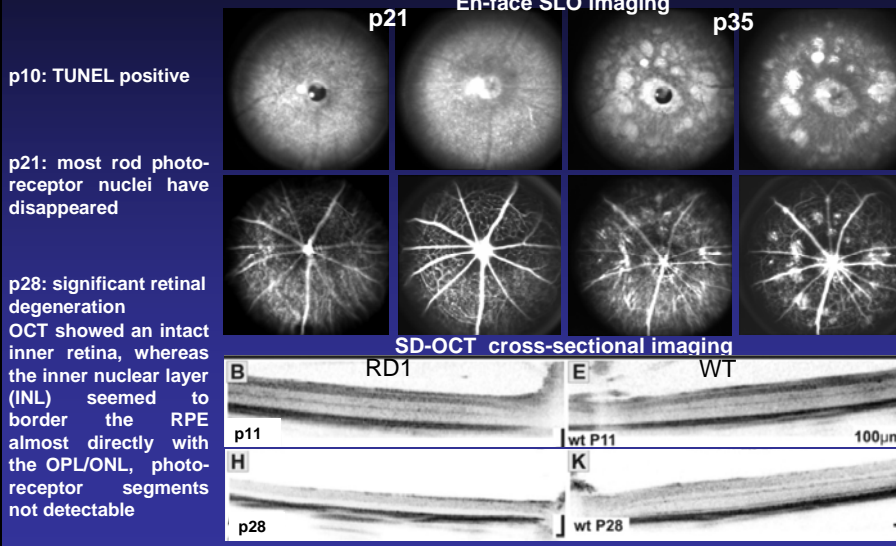
The retinoblastoma mouse model

The retinoblastoma protein (Rb) was first identified as a tumor suppressor

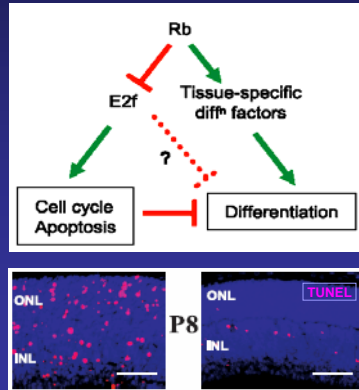Rb blocks cell division and cell death by inhibiting the E2f transcription factor family leading to apoptosis of a large fraction of retinal cells

Rb promotes differentiation into neurons by inhibition of E2f transcription factors

Rb loss has a number of systemic effects preventing the generation of knock-outs , the retinal consequences were studied in a tissue-specific Cre-lox system.

Expression of the a-Cre transgene is not topographically homogeneous in this mouse model, leading to different degrees of gene inactivation within the same organ
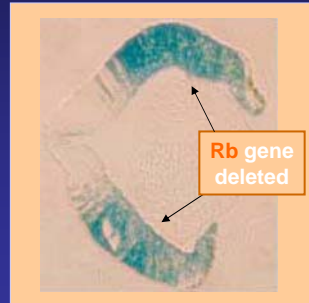

The alpha-*Cre* transgene was used to delete the floxed *Rb* exon 19. For simplicity, *Rb^{loxP/loxP};alpha-Cre* is referred to as Rb KO.

The retinoblastoma mouse model

This Cre expression pattern is reflected in retinal morphology: retinal periphery shows the full effect of Rb loss, whereas there is almost no a-Cre transgene activity in the central retina generating a distinct transition zone

An important feature of OCT is the capability to capture multiple sections directly linked to the surface image, allowing to follow topographical changes like the thickness gradient from center to periphery

A set of consecutive serial sections ("volume scan") allows topographic analysis of retinal thickness which in this case correlates with the a-Cre transgene expression in vivo.
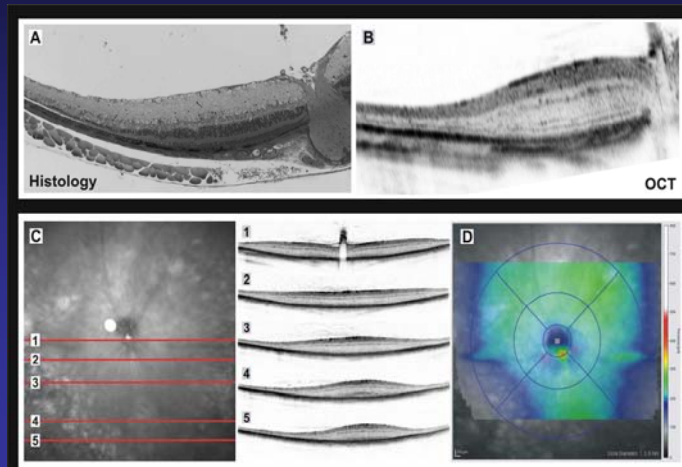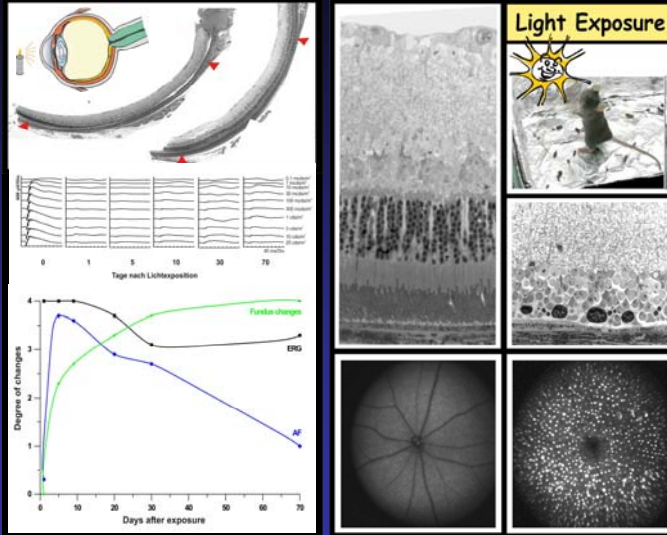
The light damage model

Light exposure inducing retinal neurodegenerations to study degenerative processes in normal retina

In this setup the mice are exposed to 5000lx for 2 hrs followed by repetitive in vivo assessment of functional and morphological changes

Already on day 1 severely reduced retinal function, weak recovery after day 30

Enhanced autofluorescence due to accumulation of lipid rich debris from degenerating photorecptors

---

The light damage model – focal exposition

Inherited retinal diseases commonly affect the retina gradually, topographical distribution of degeneration often not uniform

To mimic these conditions focal light exposure (high intensity blue light) produces strictly localized lesions adjacent to practically normal retina

allowing a direct comparison between damaged and non-damaged areas

Autofluorescent, lipid-rich debris from photoreceptor outer segments demarcates the area of damage, selective loss of the outer retina in the exposed region (asterisk) is very prominent

Transition zone closely matches that in a respective histomorphological section, but preserves the capability to follow the development of such degenerative changes over time

Novel finding: discovery of edema formation (arrow). Not visible in histology, does not endure the tissue processing. Edema was present in all (4/4) of the treated cases 3 days following the exposure, and was still present one week later (4/4). In all cases, it formed a ring around the light damage area. Edema is a common finding in human retinal diseases.
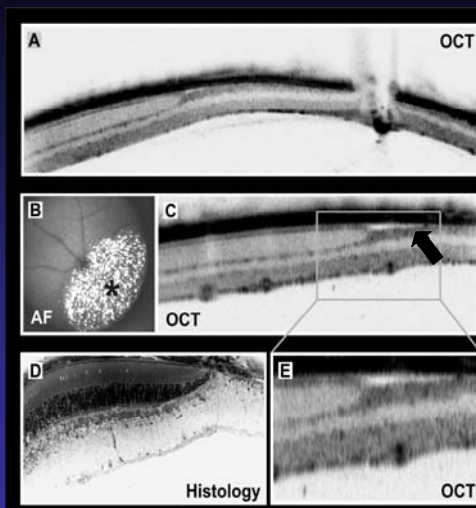
The NRL-/- mouse

In the Nrl knockout mouse, the neural retina leucine zipper (Nrl) gene is impaired

The corresponding human disease, enhanced S-cone syndrome (ESCS), may either be caused by a lack of NRL or NR2E3, a transcription factor with overlapping functions to NRL.

presenting as whitish dots in native SLO and in autofluorescence mode

The structure of lesions accessible with OCT, as before, histomorphological and OCT data correlate well. Detailed comparison illustrates the difference in image appearance between reflection- and absorption-based methods


Mears . et.al. Nat Genet
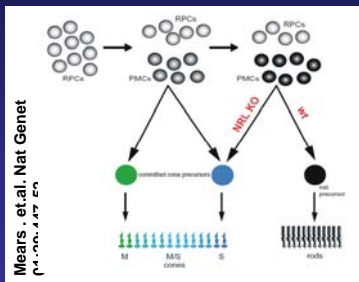
Lack of Nrl during development leads to an abnormal differentiation of rod precursors into cone-like photo-receptors

→ formation of rosettes
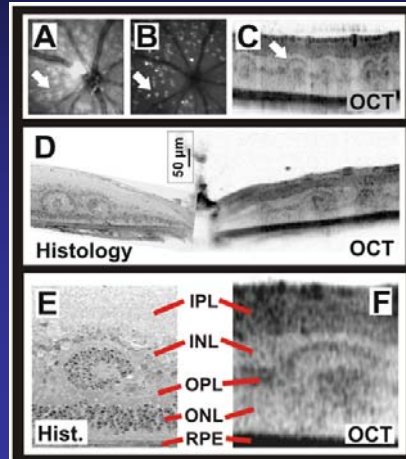
Novel rodent models for macular research

➤ Topographical differences within the retina give rise to specialized retinal regions like the macula in humans

➤ The macula is characterized by a high concentration of cones, cone bipolar cells, and ganglion cells

➤ Age-related macular degeneration (AMD) is the most common cause of untreatable blindness in the Western world

➤ Inherited maculopathies, either autosomal dominant or recessive, occur at early ages

➤ Drug toxicities, e.g. from chloroquine, can also result in complex macular degeneration

➤ Diabetic macular edema (DME) is the most common cause of vision loss in patients with diabetic retinopathy
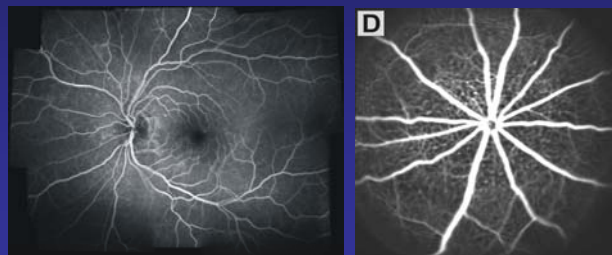
Mouse and rat do not possess a macula or even a retinal region resembling features of the macula

→ Animal models that mimic the complex and progressive characteristics of macular disorders are needed to investigate this pathophysiology and to develop specific treatment strategies

27

Animal models

Meriones unguiculatus
- „Mongolian Gerbil" or „Mongolian Jird"
- most widely known species of Gerbil subfamily
- Habitat: semi-deserts and steppes of Mongolia

Gerbillus perpallidus
- „Pallid Gerbil"
- species of Gerbil subfamily
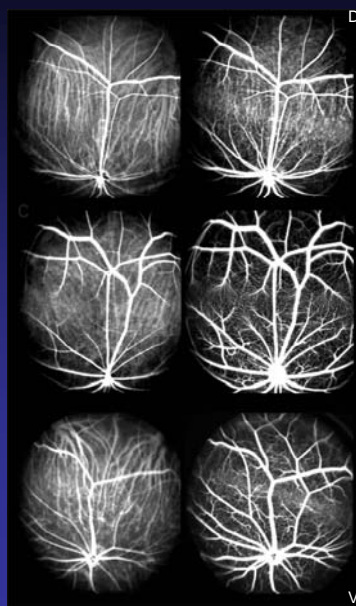- Habitat: northwestern Egypt

Phodopus campbelli
- „Campbell`s Russian dwarf hamster", „Djungarian hamster"
- species of Gerbil subfamily
- Habitat: steps and semi-arid areas of eastern and central Asia

In vivo cSLO angiography

- H-shape pattern of retinal blood vessels

- Vessels divide into several branches avoiding a distinct retinal region

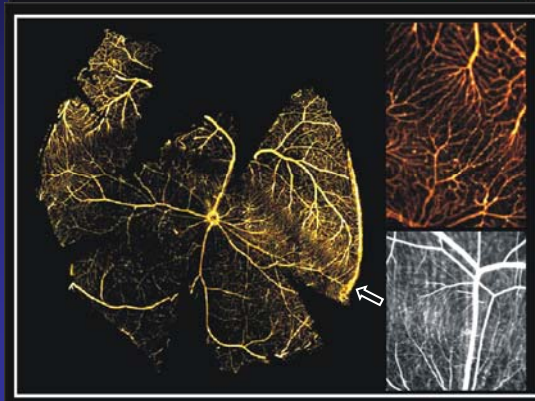- located dorsal to optic disc

specialized retinal region: visual streak

- enhanced visibility:
  FLA visualizes retinal vasculature here, choroidal vessels visible

different retinal layering

Gerbillus

Meriones

Phodopus

28

In vitro whole mount collagen IV staining – comparison to in vivo cSLO

Gerbillus perpallidus

Visual streak area

specialized vascular patterning

- in superficial vascular plexus
- reduced capillary branching
- in a horizontal band
  spanning the entire retina

- enhanced visibility

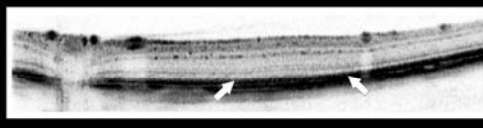different retinal layering

In vivo SD-OCT imaging

Gerbillus
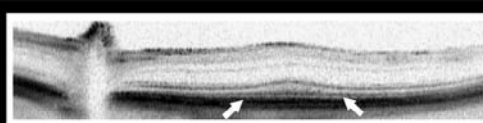
Meriones

Phodopus

Visual streak area

- increase in retinal thickness

- inner retina:
  laminar organisation unchanged

- outer retina:
  thickness increase
  in photoreceptor outer segment layer

Semithin histological sections

Gerbillus   Meriones   Phodopus
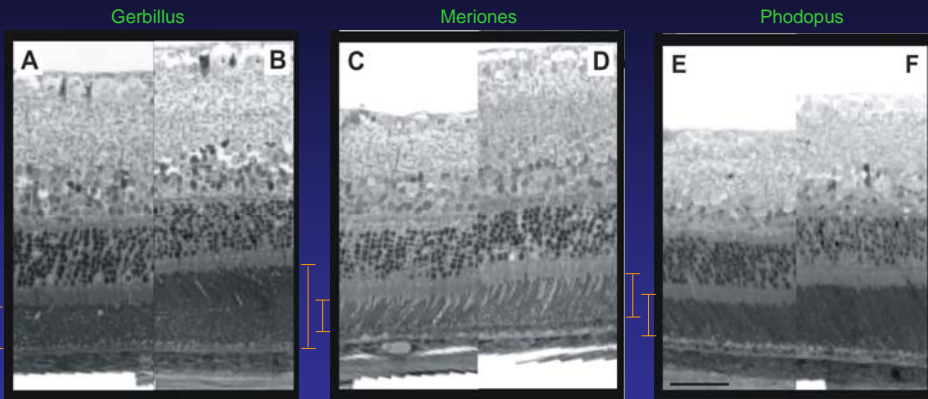
Comparison visual streak area (right) – peripheral retina (left)

- significant thickening of the retina
- photoreceptor outer segment layers enlarged

Electron microscopy

Peripheral retina

Visual streak area

photoreceptor outer segment
enlarged about 1.5 fold

generated difficulties
for embedding and cutting

slanted appeareance

Gerbillus

Nissl staining (cresyl violet) in retinal whole mount
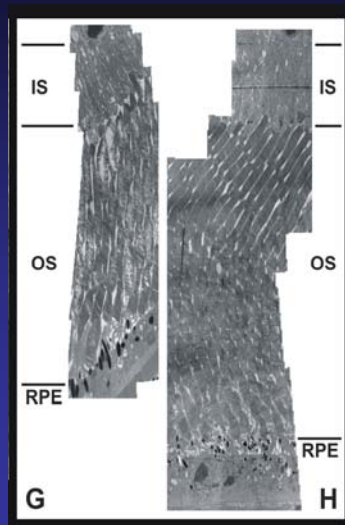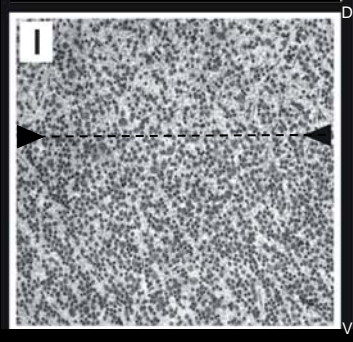
Ganglion cell layer

Gerbillus

Visual streak area

Ganglion cell streak
with enhanced neuron density

- increase sharper at the dorsal edge
- ventrally, transition more gradual

Meriones   similar distinct ganglion cell streak

Phodopus   moderate neuron cell density within the streak region

---

Cone opsin (MWS) staining in retinal whole mount

Cone cell distribution

Gerbillus

Few SWS cones, which also co-express MWS opsin,
therefore all cones are labeled

Visual streak area

Enhanced cone cell density

- increase sharper at the dorsal edge
- ventrally, transition more gradual

Meriones

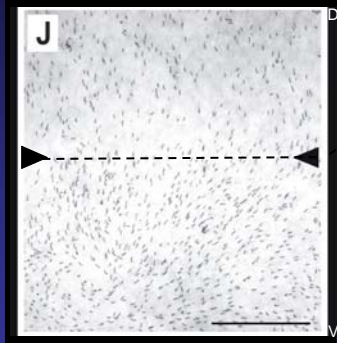**Phodopus**   enhanced cone densities across entire ventral retina

Cone densities, cone opsin expression

Interspecies differences

	Overall cone densities	Opsin expression
Gerbillus	low	mostly MWS
		few SWS, co-expressing MWS
Meriones	high	MWS/SWS expressed across the entire retina
Phodopus	high	MWS opsin expression dorsal to the streak
		SWS expression ventral

Cone opsin (MWS/SWS) expression in retinal whole mount

Phodopus

MWS

SWS

Visual streak
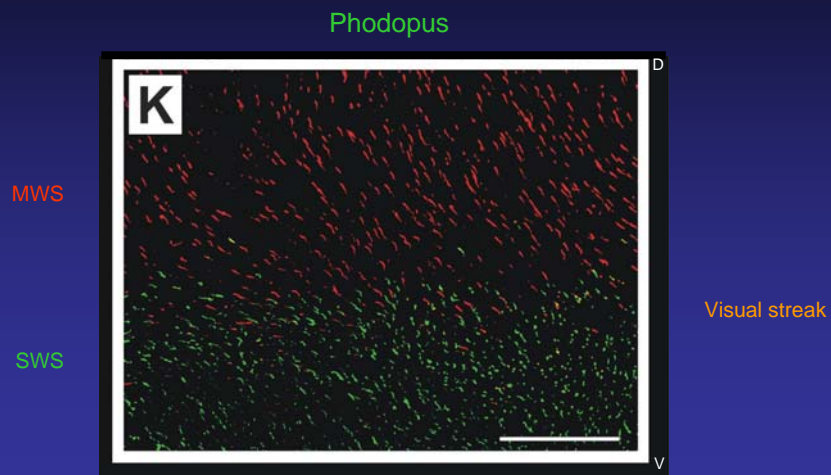
Immunofluorescence analysis of retinal sections

Dorsal periphery	Visual streak	No differences

Gerbil (Meriones)

Isolectin
Streak: sparse super-
Ficial vascular network

Meriones

SWS opsin
Streak: enhanced
cone density

Phodopus

PNA
Streak: enhanced
cone density

A   B   C   D   E   F

Meriones

GNAT1

Rod opsin

Gerbillus

MWS opsin

Nuclei contrasted with DAPI

Antibodies recognize the same antigens as in mice
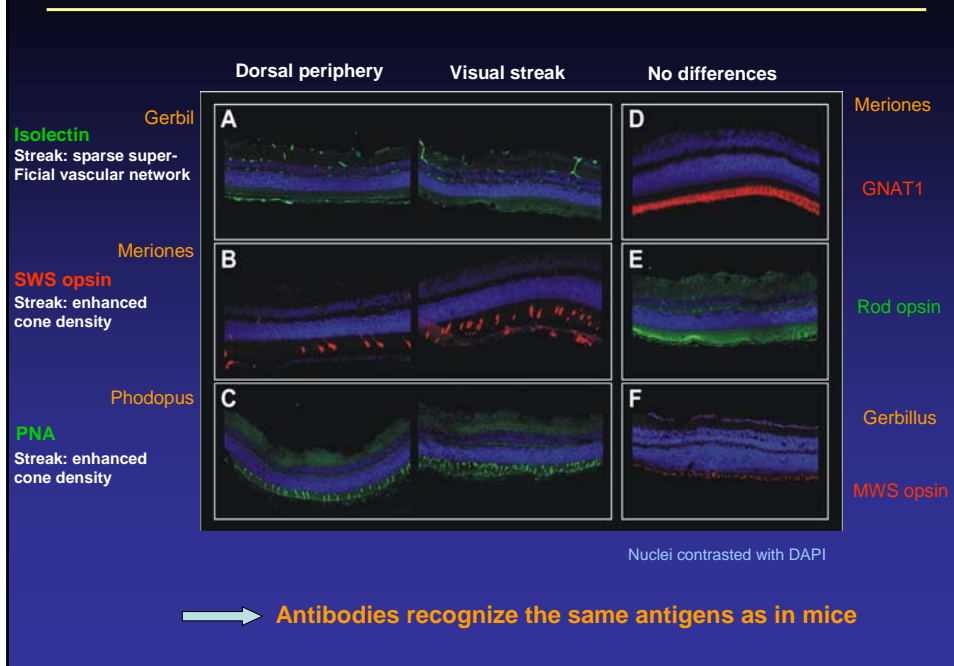
Novel rodent models for macular research - summary

Gerbillus perpallidus
Meriones unguiculatus
Phodopus campbelli

Human

Specialized retinal region — **Macula**

Sparsely vascularized area — Blood vessel and capillary free zone

Enhanced retinal thickness — Enhanced retinal thickness

Higher number of cones and ganglion cells — Higher number of cones, bipolar, ganglion cells

Conclusion

→ These small laboratory rodents present
a specialized retinal region resembling key structures of the human macula

→ Suitable model for research in macular disorders like AMD and DME

→ Development and test of therapeutic strategies

→ Inexpensive, conventional housing, easy to handle in comparison to larger animals
like cats, dogs or even primates

Non-invasive imaging techniques like scanning-laser ophthalmoscopy (SLO), and optical coherence tomography (OCT)

⟶ monitor developmental as well as inherited and induced degenerative processes

⟶ uncover the pathophysiology of ocular neurodegenerative processes

⟶ to develop and test therapeutic strategies and to understand and model normal retinal function

⟶ Repeated analysis of the same individual animals opens a wide field of applicability in future long-term and preclinical studies

⟶ In vivo techniques significantly help to reduce standard histology and thus the amount of animals needed

34